



Contents lists available at *Dergipark*

Journal of Scientific Reports-A

journal homepage: <https://dergipark.org.tr/pub/jsr-a>



E-ISSN: 2687-6167

Number 58, September 2024

RESEARCH ARTICLE

Receive Date: 17.03.2024

Accepted Date: 11.06.2024

Diffusion limited aggregation via Python: Dendritic structures and algorithmic art

Çağdaş Allahverdi^{a,*}, Yıldız Özfirat Allahverdi^b

^a*Toros University, Faculty of Engineering, Department of Software Engineering, Mezitli Campus, 33210, Mezitli, Mersin, Türkiye, ORCID: 0000-0002-6825-5099.*

^b*Mersin University, Faculty of Fine Arts, Department of Painting, Ciftlikkoy Campus, 33343, Yenişehir, Mersin, Türkiye, ORCID: 0000-0001-9794-6510*

Abstract

Diffusion limited aggregation (DLA) has attracted much attention due to its simplicity and broad applications in physics such as nano and microparticle aggregations. In this study, the algorithm of DLA is written with Python. Python's Turtle library is used to plot the aggregate on the computer monitor as it grows. The algorithm is run on the Raspberry Pi. A cheap and portable medium is created for DLA simulation. Two different options are placed in the algorithm. The first path does not allow the primary particle to turn outside of the aggregate after the collision. However, the second one allows the percolation of the primary particle both inside and outside of the aggregate. The spherical dendritic structures consisting of 500-2000 primary particles are obtained by the algorithm. The fractal dimension of these structures is around 1.68. Their porosity is found below 50%. Their gyration radii are also calculated. Beyond scientific investigation, examples of algorithmic art using these dendritic structures are also given.

© 2023 DPU All rights reserved.

Keywords: Diffusion limited aggregation; Random walk; Fractal dimension; Porosity; Raspberry Pi; Algorithmic art

* Corresponding author. Tel.: +90-324-325-3300 ; fax: +90-324-325-3301 .

E-mail address: cagdas.allahverdi@toros.edu.tr

<http://dx.doi.org/10.1016/j.cviu.2017.00.000>

1. Introduction

Diffusion limited aggregation (DLA) is the gathering of particles in random manner. DLA has an importance from the point of view of science and algorithmic art. Flocculation [1], nanoparticle aggregation [2], bacterial growth [3], Hele-Shaw fingering [4], and dielectric breakdown [5] can be imitated by using DLA. Witten and Sander generated aggregate patterns including around 3000 particles on a square lattice [6]. Woźniak et al. approximated this model to a much more realistic one [7]. Mroczka et al. derived radius of gyration and fractal dimension of silicon dioxide and soot aggregates from their light scattering intensities [8]. The effect of the number of primary particles, step length, and appearance radius on morphology and structure of aggregates was investigated by Liu et al [9]. Wang et al. compared fractal dimensions obtained from box-counting and power law methods of DLA [10]. Computer runtimes for the formation of DLA structures were studied on single and multiple CPU cores by Zsaki [11]. In DLA, only one particle moves around randomly and sticks to the targeted aggregate after colliding with it. However, many particles move around randomly, collide, and stick together in diffusion limited cluster aggregation (DLCA). Some authors studied their physical systems using DLA and DLCA [12-14].

In this study, the algorithm of DLA has been written by using Python programming language and run on Raspberry Pi 4 Model B microprocessor. Indeed, Raspberry Pi 4 is a small and low-cost single-board computer [15]. The Turtle library of Python has been used to draw sticking aggregates instantaneously on the computer monitor. Thus, DLA can be easily worked and demonstrated via this cheap equipment. The physical parameters such as fractal dimension, gyration, birth, and death radii, and working principle of the DLA have been explained in the paper. The DLA algorithm for the simulation of aggregation of non-overlapping circular (spherical at 3D) hard particles has been depicted. A mathematical explanation is given for the position adjustments of colliding circular particles. Aggregates have been grown in two different modes by keeping their fractal dimension within a certain range (1.60-1.80). These modes are i) no chance of percolation for the particle after the collision and ii) a chance of percolation for the particle after the collision. In addition, some artistic studies of these dendritic structures are given in the text.

2. Theory

The theory explained by Woźniak et al. has been taken as reference in this work [7]. However, it has been modified and the position adjustment of the particles has been clarified. In DLA, a seed particle is placed at the origin of a cartesian coordinate system. A particle is sent from a point on the perimeter of a circle at a certain distance from the center. Herein, this circle will be called birth circle, and its radius will be birth radius (R_{bi}). This particle moves randomly in the cartesian coordinate system. This is a random walk. When it collides with the seed at the center, it sticks to the seed and adjusts itself to form tangential circles. Then, another particle is sent from the birth circle. The birth radius is not constant. It is greater than the bounding radius (R_{bo}), that is $R_{bi} > R_{bo}$. The bounding radius is the radius of the circle which covers the aggregate growing from the seed. There is also a death circle. The radius of the death circle, that is death radius (R_{de}), restricts the particle movement. If the particle passes from inside to outside of the death circle, it is annihilated, and a new particle is sent from the birth circle. This process is repeated to enlarge the aggregate. Figure 1 shows this process.

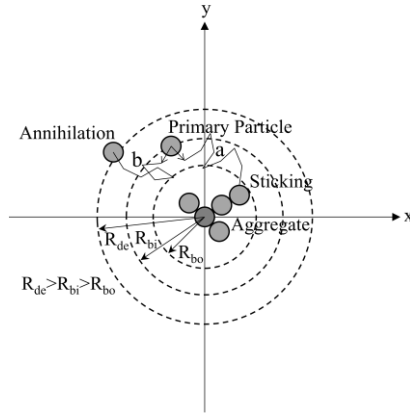


Fig. 1. Diffusion limited aggregation. Growth of the aggregate is shown by sticking. Primary particle following path a is stuck to the aggregate or following path b is annihilated. R_{de} , R_{bi} and R_{bo} are death, birth, and bounding radii, respectively.

In our aggregation growth, $R_{bi}=2.0R_{bo}$ and $R_{de}=3.0R_{bo}$ have been used. R_{bo} encircles the aggregate and can be written as in Equation 1.

$$R_{bo} = \text{maximum}(\sqrt{x_i^2 + y_i^2}) + R_0 \tag{1}$$

where x_i is the x-coordinate of i^{th} particle in the aggregate, y_i is the y-coordinate of i^{th} particle in the aggregate and R_0 is the radius of the primary particle (see Figure 2).

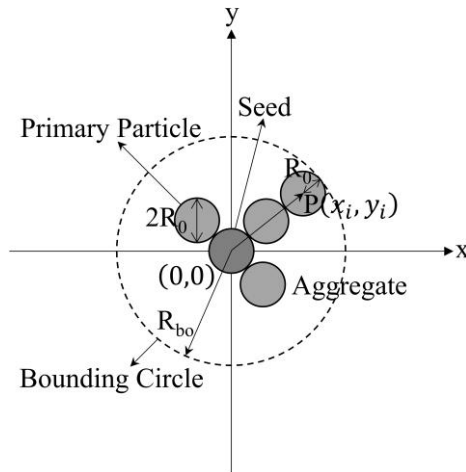


Fig. 2. Bounding circle. $P(x_i, y_i)$ shows the cartesian coordinate of the particle. R_0 and R_{bo} are the radii of the primary particle and bounding circle, respectively.

The fractal dimension (the Hausdorff dimension) of fractal structures is given by Equation 2.

$$D_f = \frac{\log\left(\frac{N}{k_0}\right)}{\log\left(\frac{R_{g,N}}{R_0}\right)} \quad (2)$$

where N is the number of primary particles, k_0 is the scaling prefactor, $R_{g,N}$ is the gyration radius and R_0 is the radius of the primary particle and D_f is the fractal dimension. $R_0=2.0$ and $N=500,1000,2000$ have been used. D_f has been kept between 1.60 and 1.80 (1.70 ± 0.10). $R_{g,N}$ has been calculated according to Equation 3.

$$R_{g,N} = \sqrt{\frac{1}{N} \sum_{i=1}^N [(x_i - x_{CM})^2 + (y_i - y_{CM})^2]} \quad (3)$$

where x_{CM} is x-coordinate of the center of mass of the aggregate and y_{CM} is y-coordinate of the center of mass of the aggregate. Assuming the primary particles are same, x_{CM} and y_{CM} are calculated using Equations 4 and 5, respectively.

$$x_{CM} = \frac{\sum_{i=1}^N m_0 x_i}{\sum_{i=1}^N m_0} = \frac{1}{N} \sum_{i=1}^N x_i \quad (4)$$

$$y_{CM} = \frac{\sum_{i=1}^N m_0 y_i}{\sum_{i=1}^N m_0} = \frac{1}{N} \sum_{i=1}^N y_i \quad (5)$$

where m_0 is the mass of the primary particle.

The colliding two particles can be made tangential by using the equations of analytic geometry in the 2D Euclidean space. Figure 3 shows colliding and position adjustment of two primary particles. They will be called particle 1 and particle 2. Particle 1 is randomly moving individual particle and particle 2 is a primary particle of the aggregate. x_{1a} , x_1 , y_{1a} , y_1 , x_2 , y_2 , and θ are adjusted x-coordinate of particle 1, x-coordinate of particle 1 before the adjustment, adjusted y-coordinate of particle 1, y-coordinate of particle 1 before the adjustment, x-coordinate of particle 2, y-coordinate of particle 2, and the angle of incidence of particle 1 respectively.

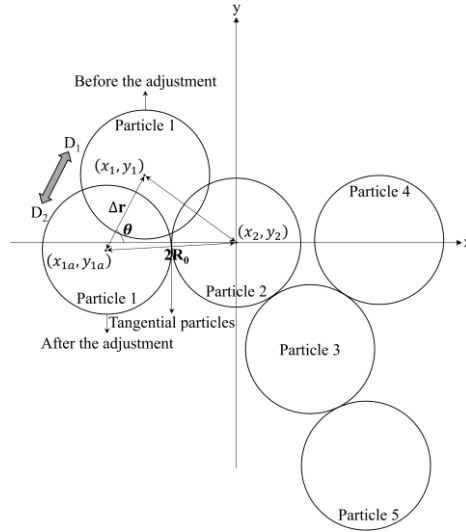


Fig. 3. Adjustment of the position of particle 1 relative to the aggregate. Particles 2, 3, 4, and 5 are the member particles of the aggregate. After the collision of particle 1 with particle 2, particle 1 is moved by Δr in the direction of D_2 . Particle 1 and particle 2 are tangential to each other and particle 1 becomes a new member of the aggregate. $2R_0$ is the diameter of the particle.

As seen from Figure 3, the distance between the centers of particle 1 and particle 2 after the adjustment must be $2R_0$. Equation 6 indicates that particle 1 and particle 2 are tangential.

$$(x_{1a} - x_2)^2 + (y_{1a} - y_2)^2 = 4R_0^2 \quad (6)$$

Equation of the line connecting the center of particle 1 before the adjustment to the center of particle 1 after the adjustment is written as follows.

$$y(x) = mx + n = (\tan\theta)x + n \quad (7)$$

where m is the slope of the line and n is the y -intercept of the line. (x_{1a}, y_{1a}) and (x_1, y_1) coordinates satisfy Equation 7.

$$y_{1a} = (\tan\theta)x_{1a} + n \quad (8)$$

$$y_1 = (\tan\theta)x_1 + n \quad (9)$$

$$n = y_1 - (\tan\theta)x_1 \quad (10)$$

If Equation 8 is written in Equation 6 and Equation 6 is arranged in the form of quadratic equation, Equation 11 is obtained.

$$(1 + \tan^2 \theta)x_{1a}^2 + 2(n \tan\theta - x_2 - y_2 \tan\theta)x_{1a} + (x_2^2 + y_2^2 + n^2 - 2ny_2 - 4R_0^2) = 0 \quad (11)$$

Herein, the solution of Equation 11 is given as follows.

$$a = 1 + \tan^2 \theta \quad (12)$$

$$b = 2(n \tan \theta - x_2 - y_2 \tan \theta) \quad (13)$$

$$c = x_2^2 + y_2^2 + n^2 - 2ny_2 - 4R_0^2 \quad (14)$$

$$x_{1a} = \frac{-b \pm \sqrt{b^2 - 4ac}}{2a} \quad (15)$$

x_{1a} can be calculated using Equation 15. Equation 15 gives two solutions, but the displacement from (x_{1a}, y_{1a}) and (x_1, y_1) must be equal or smaller than the step length of the particle 1 which is $2R_0$ in this study. Therefore, the solution satisfying Equations 16, 17 and 18 is chosen. Here, n and y_{1a} are calculated by Equations 10 and 8.

$$\Delta r = \sqrt{(x_{1a} - x_1)^2 + (y_{1a} - y_1)^2} \leq 2R_0 \quad (16)$$

$$x_{prev} < x_{1a} < x_1 \quad (17)$$

$$y_{prev} < y_{1a} < y_1 \quad (18)$$

where x_{prev} and y_{prev} are previous x and y coordinates of particle 1 before the collision between particle 1 and particle 2. (x_{1a}, y_{1a}) gives the adjusted position of particle 1. The center of particle 1 is moved from (x_1, y_1) to (x_{1a}, y_{1a}) . Thus, sticky (tangential) primary particles are generated. The porosity of the agglomerate can be calculated as follows.

$$V_f = 1 - N \left(\frac{R_0}{R_{g,N}} \right)^2 \quad (19)$$

The algorithm of the DLA used in this study is indicated in Figure 4. The data involves $R_{g,N}$ and D_f of the agglomerate in the flow diagram. Numbers 1 and 2 show two different aggregation modes. If the position of the collided particle cannot be adjusted relative to the agglomerate, there are two ways to follow. The collided particle is annihilated, and a new particle is sent from the circle of the birth for way 1. However, the collided particle is moved and not annihilated for way 2. These ways are called mode 1 and mode 2 below.

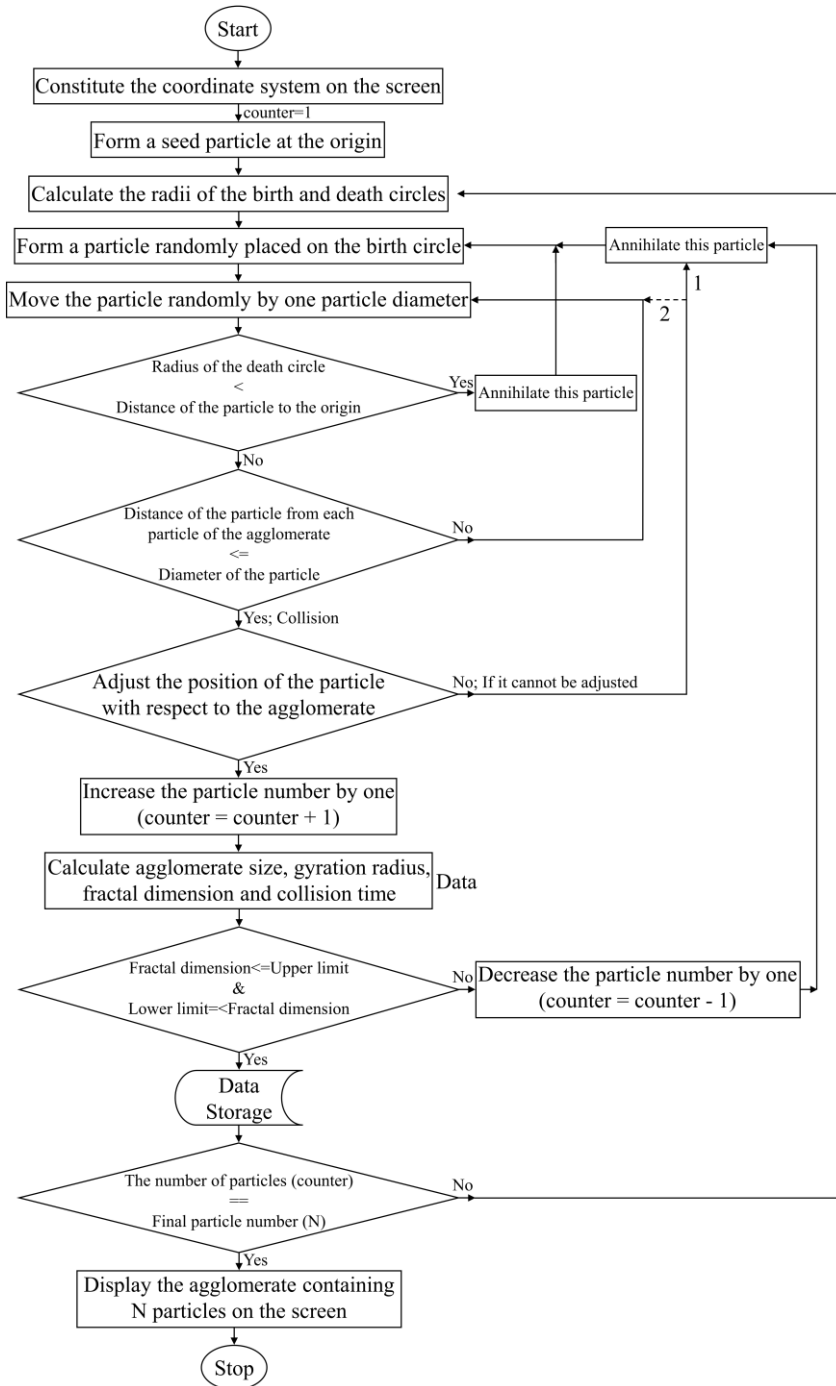


Fig. 4. The flowchart of the DLA. 1 and 2 show two different paths which are called mode 1 and mode 2 in the text, respectively.

3. Equipment

The equipment used in this study is given in Table 1. As understood from Table 1, the listed items are easy to reach and relatively cheap. Figure 5 shows this equipment.

Table 1. The equipment used for the DLA simulation.

No	Item	Quantity
1	Raspberry Pi 4 Model B (64-bit quad-core Cortex-A72 processor)	1
2	FASTER 64 GB Micro SD Card	1
3	Aluminum case with dual cooling fan for Raspberry Pi 4	1
4	Raspberry Pi DC 5.1V/3A output USB-C Power Supply	1
5	ACER v193w 19-inch LCD monitor coupled with VGA cable and power cord	1
6	Micro-HDMI to HDMI cable	1
7	HDMI to VGA and Audio adapter	1
8	POWERFUL SLE-650 650VA Line Interactive UPS	1
9	TRUST VEZA wireless multimedia keyboard with touchpad	1



Fig. 5. The equipment used for the DLA simulation. The numbers correspond to the parts of the equipment given in Table 1.

4. Results and Discussion

Figure 6 shows the generated aggregates consisting of 500, 1000 and 2000 primary particles via mode 1. As seen from Figure 6, these are dendritic structures (tree-like structures) [16, 17] and are called $D1_{500}$, $D1_{1000}$ and $D1_{2000}$.

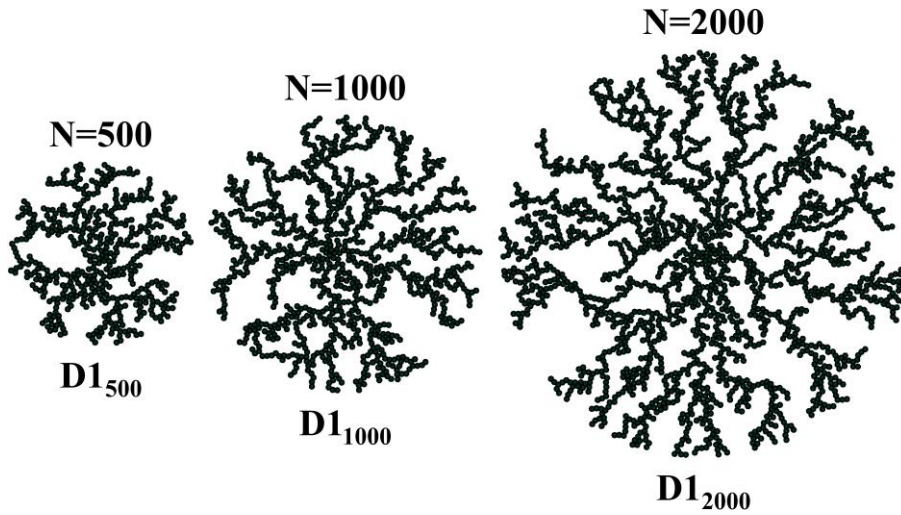


Fig. 6. The dendritic structures generated by the DLA. $D1_{500}$, $D1_{1000}$ and $D1_{2000}$ indicate the dendritic structures consisting of 500, 1000 and 2000 particles, respectively. These structures are generated with mode 1.

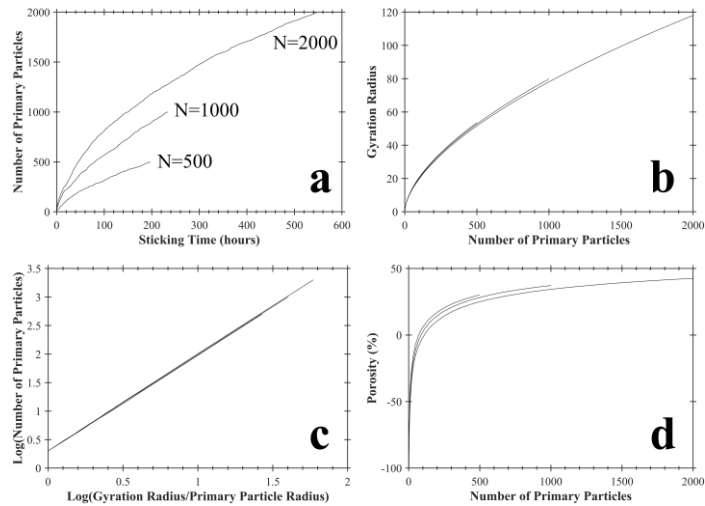


Fig. 7. The plots obtained from $D1_{500}$, $D1_{1000}$ and $D1_{2000}$. a) Number of primary particles versus sticking time, b) Gyration radius versus number of primary particles, c) Log(number of primary particles) versus log(gyration radius/primary particle radius) and d) Porosity versus number of primary particles. The slope gives D_f in Figure 7c.

The plots obtained for these structures are given in Figure 7. $D1_{500}$, $D1_{1000}$ and $D1_{2000}$ are formed at the end of 197 h, 234 h and 546 h, respectively (see Figure 7a). Larger structures need more primary particles, and more particles require more time to form the structure. Their gyration radii evolution is similar (see Figure 7b). It means that the generated structures are analogous. The radii of gyration of $D1_{500}$, $D1_{1000}$ and $D1_{2000}$ are found to be 54, 80, and 118, respectively. Figure 7c shows plot of $\text{Log}(N)$ versus $\text{Log}(R_g/R_0)$. According to Equation (2), the slope and y-intercept of the linear line in Figure 7c give D_f and $\text{Log}(k_0)$ of the agglomerate, respectively. The fractal dimensions (D_f) of $D1_{500}$, $D1_{1000}$ and $D1_{2000}$ are 1.69, 1.68 and 1.68, respectively. The scaling prefactors (k_0) of $D1_{500}$, $D1_{1000}$ and $D1_{2000}$ are 1.95, 2.04 and 2.10, respectively. Figure 7d indicates the porosities. The porosities (V_f) of $D1_{500}$, $D1_{1000}$ and $D1_{2000}$ are found to be 30%, 37% and 43%, respectively. As the structure grows, porosity increases, but the increment gradually slows down. The aggregate generated via mode 2 is shown in Figure 8. It contains 2000 primary particles. It is called $D2_{2000}$. It is formed at the end of 710 h. D_f , R_g , and V_f of $D2_{2000}$ are 1.68, 124 and 48%, respectively. $D2_{2000}$ is larger and more porous than $D1_{2000}$. This result can be understood. The primary particle moves inside and outside of the aggregate until it finds a suitable location for sticking. Therefore, as in Figure 8, mode 2 can form a more porous structure than mode 1.

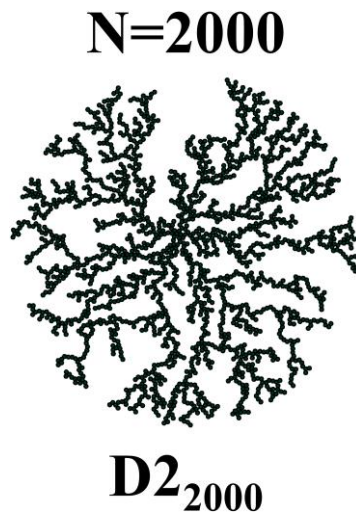


Fig. 8. The dendritic structure generated by using mode 2 of the DLA. It consists of 2000 particles. It is called $D2_{2000}$.

As a result of the combustion of fossil fuels, soot particles are released into the environment. These soot aggregates give rise to global warming due to the absorption and scattering of sunlight. Soot aggregates are shown to have a fractal morphology. This morphology has an impact on their light scattering properties. Hence, the fractal properties of these structures have been investigated by using transmission electron microscopy. For instance, Pang et al. examined different soot aggregates originated from combustion of fuel, burning biomass, and burning coal [18]. D_f values between 1.11-2.19 with k_0 values between 0.25-9.22 were reported for the soot aggregates in the literature [18-21]. Our findings are within these ranges obtained from literature studies. Unlike the studies in literature, porosity has been calculated in this work. The sticking probability of the primary particles is taken as ~ 1.0 when the algorithm is run. Compact and denser dendritic structures can be generated by defining a sticking probability parameter which is sufficiently smaller than 1.0 in the algorithm. These results are not limited by the soot aggregates and can be expanded to the other natural fractal structures such as manganese dendrites formed on magnesium silicate [22].

5. Algorithmic Art

Algorithmic art is a form of art that uses algorithms. Nowadays, all algorithms are nearly computer algorithms. A computer algorithm consists of computer code written to perform a specific task. Algorithmists use these computer algorithms to perform their arts. Manfred Mohr, Jean-Pierre Hébert, Vera Molnár and Roman Verostko are among famous algorithmists [23]. For example, Manfred Mohr uses the edge sets of a cube very well in his works [24].

The dendritic structures created in this study by the DLA algorithm are valuable not only in point of the science but also in terms of algorithmic art. Here, the final pattern can be predicted but it cannot be fully known as the final work of an artist's painting. It is caused by the randomness used in the algorithm. Hence each DLA pattern is unique. Some artistic colorings of $D1_{2000}$ are shown in Figure 9. The primary particles of $D1_{2000}$ are colored from inside to outside by using three different colors and shown on a circular area surrounding it. The circular area is colored in six different colors. All colors in the RGB color palette can be used in the dendritic structure. Other geometric shapes may also be preferred instead of circular area. The size of primary particles is reduced in Figure 10.

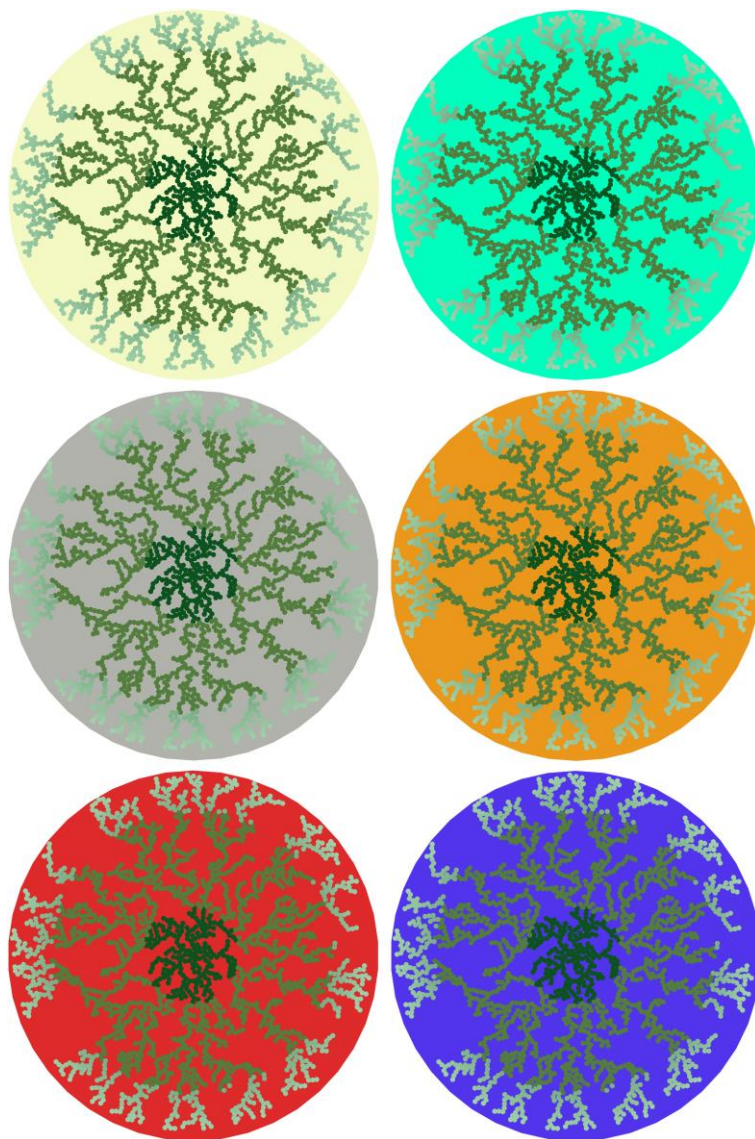


Fig. 9. Colored $D1_{2000}$.

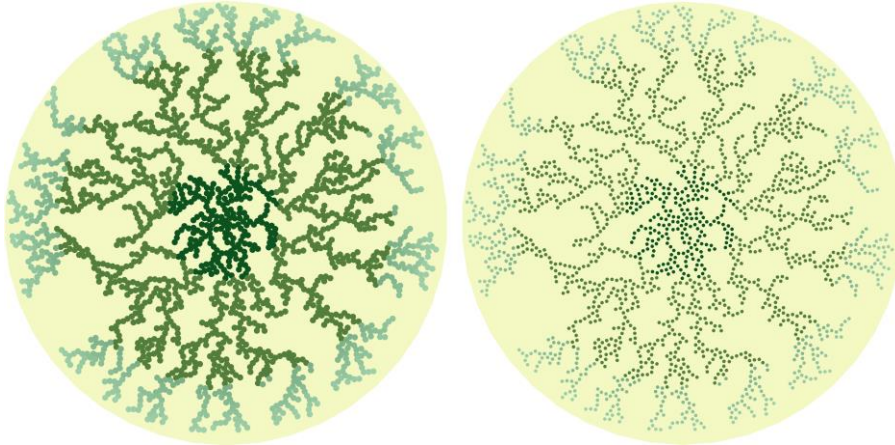


Fig. 10. Colored and reduced primary particles of D1₂₀₀₀.

6. Conclusion

The algorithm of DLA is written via Python and it runs on the Raspberry Pi. Turtle library is used to draw the aggregate on the screen. Thus, cheap and portable virtual exhibition platform is created for DLA. Such an exhibition is valuable for classroom and scientific demonstrations and digital exhibitions. Percolation of primary particles towards inside and outside of the aggregate is also considered in the algorithm. Spherical dendritic structures are generated. The fractal dimension of these structures is around 1.68. The porosity increases with the number of primary particles participated to the aggregate, but it is found below 50% for these structures consisting of 2000 particles. The dendritic structures are used for artistic studies. These works are among examples of algorithmic art. Unlimited artworks can be produced by using these dendritic structures.

Acknowledgements

The authors would like to thank Toros University for the financial assistance provided for the successful completion of this study.

References

- [1] J. Nan, M. Yao, T. Chen, Z. Wang, Q. Li and D. Zhan, "Experimental and numerical characterization of floc morphology: role of changing hydraulic retention time under flocculation mechanisms", *Environ. Sci. Pollut. Res.*, vol. 23, pp. 3596-3608, 2016, doi: 10.1007/s11356-015-5539-7.
- [2] B. Lim and Y. Xia, "Metal nanocrystals with highly branched morphologies", *Angew. Chem. Int. Ed.*, vol. 50, no. 1, pp. 76-85, 2011, doi: 10.1002/anie.201002024.
- [3] H. Tronolone *et al.*, "Diffusion-limited growth of microbial colonies", *Sci. Rep.*, vol. 8, pp. 1-11, 2018, doi: 10.1038/s41598-018-23649-z.
- [4] J. Zhang, J. Luo and Z. Liu, "DLA simulation with sticking probability for viscous fingering", in *2011 International Conference on Consumer Electronics, Communications and Networks (CECNet)*, Xianning, China, 2011, pp. 4044-4047, doi: 10.1109/CECNET.2011.5768540.
- [5] I. M. Irurzun, P. Bergero, V. Mola, M. C. Cordero, J. L. Vicente and E. E. Mola, "Dielectric breakdown in solids modeled by DBM and DLA", *Chaos, Solitons and Fractals*, vol. 13, no. 6, pp. 1333-1343, 2002, doi: 10.1016/S0960-0779(01)00142-4.
- [6] T. A. Witten and L. M. Sander, "Diffusion-limited aggregation", *Phys. Rev. B*, vol. 27, no. 9, pp. 5686-5697, 1983, doi: 10.1103/PhysRevB.27.5686.

- [7] M. Wozniak, F. R. A. Onofri, S. Barbosa, J. Yon and J. Mroczka, "Comparison of methods to derive morphological parameters of multi-fractal samples of particle aggregates from TEM images", *J. Aerosol Sci.*, vol. 47, pp. 12-26, 2012, doi: 10.1016/j.jaerosci.2011.12.008.
- [8] J. Mroczka, M. Woźniak and F. R. A. Onofri, "Algorithms and methods for analysis of the optical structure factor of fractal aggregates", *Metrol. Meas. Syst.*, vol. XIX, no. 3, pp. 459-470, 2012, doi: 10.2478/v10178-012-0039-2.
- [9] D. Liu, W. Zhou, Z. Qiu and X. Song, "Fractal simulation of flocculation processes using a diffusion-limited aggregation model", *Fractal Fract.*, vol. 1, pp. 1-13, 2017, doi: 10.3390/fractalfract1010012.
- [10] R. Wang, A. K. Singh, S. R. Kolan and E. Tsotsas, "Fractal analysis of aggregates: correlation between the 2D and 3D box-counting fractal dimension and power law fractal dimension", *Chaos, Solitons and Fractals*, vol. 160, pp. 1-13, 2022, doi: 10.1016/j.chaos.2022.112246.
- [11] A. M. Zsaki, "Hardware-accelerated generation of 3D diffusion-limited aggregation structures", *J. Parallel Distrib. Comput.*, vol. 97, pp. 24-34, 2016, doi: 10.1016/j.jpdc.2016.06.009.
- [12] N. H. Borzęcka, B. Nowak, R. Pakuła, R. Przewodzki and J. M. Gac, "Cellular automata modeling of silica aerogel condensation kinetics", *Gels*, vol. 7, pp. 1-12, 2021, doi: 10.3390/gels7020050.
- [13] M. Polimeno, C. Kim and F. Blanchette, "Toward a realistic model of diffusion-limited aggregation: rotation, size-dependent diffusivities, and settling", *ACS Omega*, vol. 7, no. 45, pp. 40826-40835, 2022, doi: 10.1021/acsomega.2c03547.
- [14] O. Tomchuk, "Models for simulation of fractal-like particle clusters with prescribed fractal dimension", *Fractal Fract.*, vol. 7, pp. 1-25, 2023, doi: 10.3390/fractalfract7120866.
- [15] S. J. Johnston and S. J. Cox, "The Raspberry Pi: a technology disrupter, and the enabler of dreams", *Electronics*, vol. 6, pp. 1-7, 2017, doi: 10.3390/electronics6030051.
- [16] N. Liu *et al.*, "Dynamic mechanism of dendrite formation in Zhoukoudian, China", *Appl. Sci.*, vol. 13, pp. 1-10, 2023, doi: 10.3390/app13042049.
- [17] D. D. Ruzhitskaya, S. B. Ryzhikov and Y. V. Ryzhikova, "Features of self-organization of objects with a fractal structure of dendritic geometry", *Moscow Univ. Phys.*, vol. 76, no. 5, pp. 253-263, 2021, doi: 10.3103/S0027134921050143.
- [18] Y. Pang *et al.*, "Quantifying the fractal dimension and morphology of individual atmospheric soot aggregates", *J. Geophys. Res. Atmos.*, vol. 127, no. 5, pp. 1-11, 2022, doi: 10.1029/2021JD036055.
- [19] A. M. Brasil, T. L. Farias and M. G. Carvalho, "Evaluation of the fractal properties of cluster-cluster aggregates", *Aerosol Sci. Tech.*, vol. 33, no. 5, pp. 440-454, 2000, doi: 10.1080/02786820050204682.
- [20] Ü. Ö. Köylü, G. M. Faeth, T. L. Farias and M. G. Carvalho, "Fractal and projected structure properties of soot aggregates", *Combustion and Flame*, vol. 100, no. 4, pp. 621-633, 1995, doi: 10.1016/0010-2180(94)00147-K.
- [21] N. Doner and F. Liu, "Impact of morphology on the radiative properties of fractal soot aggregates", *J. Quant. Spectrosc. Radiat. Transf.*, vol. 187, pp. 10-19, 2017, doi: 10.1016/j.jqsrt.2016.09.005.
- [22] Z. Merdan and M. Bayirli, "Computation of the fractal pattern in manganese dendrites", *Chinese Phys. Lett.*, vol. 22, no. 8, pp. 2112-2115, 2005, doi: 10.1088/0256-307X/22/8/080.
- [23] V. Ceric, "Algorithmic art: technology, mathematics and art", in *ITI 2008, 30th International Conference on Information Technology Interfaces*, Cavtat, Croatia, 2008, pp. 75-82, doi: 10.1109/ITI.2008.4588386.
- [24] A. Daudrich, "Algorithmic art and its art-historical relationships", *Journal of Science and Technology of The Arts*, vol. 8, no. 1, pp. 37-44, 2016, doi: 10.7559/citarj.v8i1.220.